

Chapter 2

A Zinc(II) Phthalocyanine Conjugated with an Oxaliplatin Derivative for Dual Chemo- and Photodynamic Therapy

2.1 Introduction

As mentioned in [Chap. 1](#), there has been considerable interest in combining photodynamic therapy (PDT) with other anticancer therapeutic methods. The combination of modalities that act on different disease pathways has shown several advantages, such as enhanced therapeutic efficacy, reduced side effects, and retarded drug-resistance problem [1]. For dual PDT and chemotherapy, there are generally three approaches, including sequential administration of a photosensitizer and an anticancer drug, the use of their covalent and non-covalent conjugates, and co-encapsulation of these agents in a polymeric nanocarrier. For some of the cases, additive or synergistic effects have been observed which can reduce the effective doses of anticancer drugs.

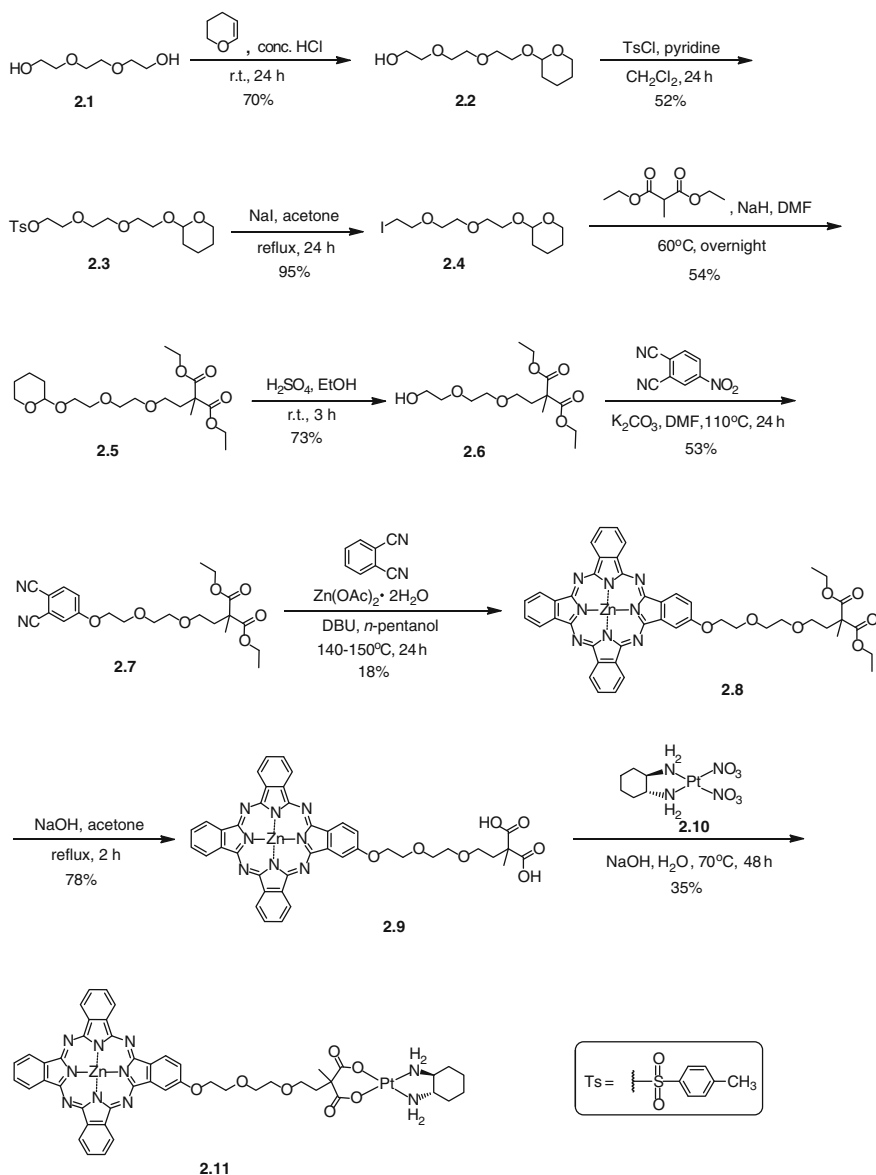
In light of the potential advantages of combined chemo- and PDT, we have been interested in studying phthalocyanine-based photosensitizers conjugated with platinum-based anticancer drugs. The latter have been widely used for the treatment of a variety of cancers through disruption of DNA in the nucleus [2, 3]. It is believed that the combination of these two components can embrace the advantages of the two very different therapeutic mechanisms and the resulting conjugates can exhibit synergistic anticancer effects. In this chapter, we report the preparation and in vitro photodynamic activities of such a conjugate, in which an oxaliplatin derivative is linked to a zinc(II) phthalocyanine core through a triethylene glycol spacer. The conjugate is highly potent of which the cytotoxicity is five-fold higher than that of the analogue without the platinum complex, demonstrating the cooperative effects of the two cytotoxic components.

2.2 Results and Discussion

2.2.1 Molecular Design, Synthesis, and Characterization

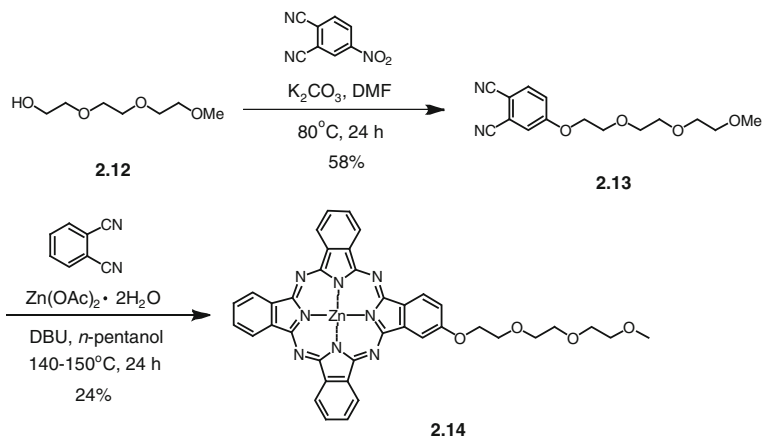
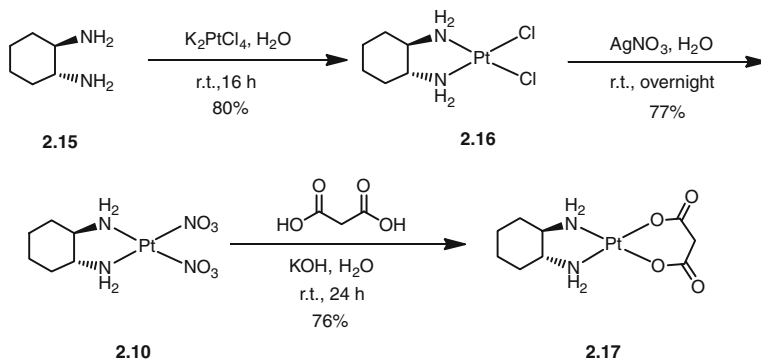
In this conjugate, a zinc(II) phthalocyanine was employed as the photosensitizing unit due to its near-infrared fluorescence emission, high singlet oxygen generation efficiency, and high photostability [4–6]. Owing to the high therapeutic efficacy of oxaliplatin [2, 3, 7] a derivative of this drug was selected as the cytostatic part. The two components were linked with a triethylene glycol chain, which can enhance the amphiphilicity and biocompatibility of the system. Scheme 2.1 shows the synthetic route used to prepare this conjugate. Starting with the commercially available triethylene glycol (**2.1**), protection of one of the hydroxyl groups with 3,4-dihydropyran under an acidic condition afforded 2-[2-(2-(tetrahydropyranyloxy)ethoxy)ethoxy]-ethanol (**2.2**) [8]. This compound was then tosylated to give compound **2.3** [8], followed by substitution with sodium iodide in refluxing acetone to give 1-iodo-8-(tetrahydro-2*H*-pyran-2-yloxy)-3,6-dioxaoctane (**2.4**) [9]. It was then reacted with diethyl methylmalonate in the presence of NaH in *N,N*-dimethylformamide (DMF) to give compound **2.5**. The tetrahydropyranyl protecting group of **2.5** was then removed with concentrated sulfuric acid to give compound **2.6**. Nucleophilic aromatic substitution reaction of 4-nitrophthalonitrile with alcohol **2.6** afforded the substituted phthalonitrile **2.7**. This compound then underwent mixed cyclization with an excess of 1,2-dicyanobenzene in the presence of $\text{Zn}(\text{OAc})_2 \cdot 2\text{H}_2\text{O}$ and 1,8-diazabicyclo [5.4.0] undec-7-ene (DBU) in *n*-pentanol to give the “3 + 1” unsymmetrical phthalocyanine **2.8** in 18 % yield. This compound was then hydrolyzed with NaOH in acetone to yield the carboxyl derivative **2.9**, which was further complexed with *trans*-(*d,l*)-1,2-diaminocyclohexanedinitratoplatinum(II) (**2.10**) [10] in an aqueous NaOH solution to give the phthalocyanine-platinum complex conjugate **2.11**. This compound was purified by flash column chromatography followed by recrystallization from a mixture of DMF and ethanol.

For comparison, two model compounds, phthalocyanine **2.14** and oxaliplatin analogue **2.17**, were also prepared. Scheme 2.2 shows the preparation of phthalocyanine **2.14**. Treatment of triethylene glycol monomethyl ether (**2.12**) with 4-nitrophthalonitrile in the presence of anhydrous potassium carbonate in DMF gave 4-(3,6,9-trioxadecyloxy)phthalonitrile (**2.13**) [11]. It was then treated with an excess of 1,2-dicyanobenzene and $\text{Zn}(\text{OAc})_2 \cdot 2\text{H}_2\text{O}$ to afford the β -substituted phthalocyanine **2.14**. Scheme 2.3 shows the synthetic route for the preparation of oxaliplatin analogue **2.17**. *Trans*-(*d,l*)-1,2-diaminocyclohexane (**2.15**) underwent a ligand substitution reaction with potassium tetrachloroplatinate(II) in water to give dichloroplatinum(II) complex **2.16** in good yield. Silver nitrate was then used to precipitate the two chloro ligands to obtain dinitratoplatinum(II) complex **2.10**. *Trans*-(*d,l*)-1,2-diaminocyclohexane-malonatoplatinum(II) (**2.17**) was prepared by treating **2.10** with an aqueous solution of malonic acid and KOH [10]. All the new



Scheme 2.1 Synthesis of phthalocyanine-platinum complex conjugate **2.11**

compounds were fully characterized with various spectroscopic methods and elemental analysis (for phthalocyanines **2.9**, **2.11**, and **2.14**) or accurate mass measurements (for phthalocyanine **2.8** and all the precursors).

Scheme 2.2 Synthesis of phthalocyanine **2.14**Scheme 2.3 Synthesis of *trans*-(d,l)-1,2-diaminocyclohexanemalonatoplatinum(II) (**2.17**)

2.2.2 Electronic Absorption and Photophysical Properties

The absorption spectrum of **2.11** in DMF was typical as the spectra for non-aggregated phthalocyanines (Fig. 2.1). It showed a B-band at 344 nm, two vibronic bands at 607 and 639 nm, and an intense and sharp Q-band at 672 nm, which strictly followed the Lambert–Beer’s law. Upon excitation at 610 nm, the compound showed a fluorescence emission at 688 nm with a fluorescence quantum yield (Φ_F) of 0.22 relative to the unsubstituted zinc(II) phthalocyanine (ZnPc) ($\Phi_F = 0.28$) [12]. The spectral data of the reference compound **2.14** were very similar to those of **2.11**, except its slightly higher value of Φ_F (0.25) probably due to the absence of the heavy platinum complex (Fig. 2.2 and Table 2.1).

To evaluate the photosensitizing efficiency of these two compounds, their singlet oxygen quantum yields (Φ_Δ) were determined in DMF by a steady-state

Fig. 2.1 Electronic absorption spectra of **2.11** in DMF in different concentrations. The inset plots the absorbance at 672 nm versus the concentration of **2.11**

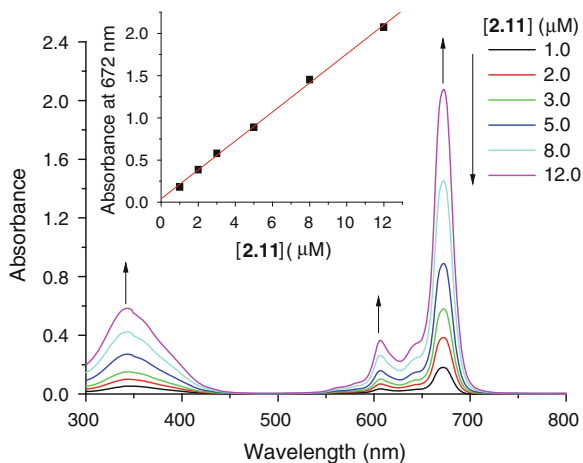


Fig. 2.2 Electronic absorption spectra of **2.14** in DMF in different concentrations. The inset plots the absorbance at 672 nm versus the concentration of **2.14**

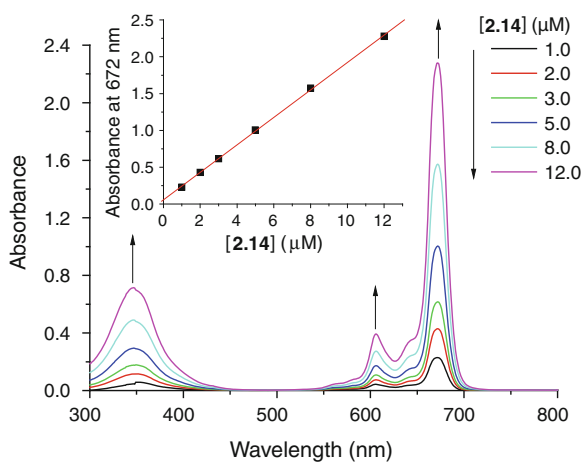


Table 2.1 Electronic absorption and photophysical data for **2.11** and **2.14** in DMF

Compound	λ_{\max} (nm) ($\log \epsilon$)	λ_{em} (nm) ^a	Φ_{F} ^b	Φ_{Δ}^{c}
2.11	344 (4.69), 607 (4.48), 639 (4.42), 672 (5.23)	688	0.22	0.56
2.14	347 (4.78), 606 (4.50), 639 (4.42), 672 (5.27)	688	0.25	0.57

^a Excited at 610 nm

^b Using ZnPc in DMF as the reference ($\Phi_{\text{F}} = 0.28$)

^c Using ZnPc as the reference ($\Phi_{\Delta} = 0.56$ in DMF)

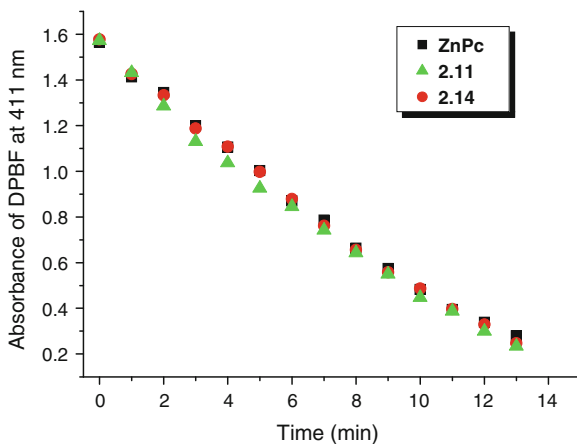
method with 1,3-diphenylisobenzofuran (DPBF) as the scavenger. The concentration of the quencher was monitored spectroscopically at 411 nm with time of irradiation (Fig. 2.3), from which the values of Φ_{Δ} could be determined by the

method described previously [13]. The results showed that both compounds are highly efficient singlet oxygen generators and the values of Φ_{Δ} were virtually identical to that of ZnPc ($\Phi_{\Delta} = 0.56$) (Table 2.1).

2.2.3 In Vitro Photodynamic Activities

The cytotoxic effects of conjugate **2.11** in a Cremophor EL emulsion were then investigated. The surfactant was added to solubilize the compound in water and reduce its aggregations. Since oxaliplatin is one of the most important chemotherapeutic drugs in colorectal cancer treatment [7], HT29 human colon adenocarcinoma cells were used for these studies. In order to reveal the photo- and chemo-cytotoxic effects of **2.11**, the antiproliferative properties of the two reference compounds **2.14** and **2.17** were also examined. Figure 2.4 shows the dose-dependent survival curves for these compounds. It can be seen in Fig. 2.4a that the non-platinum-containing phthalocyanine **2.14** does not show any dark toxicity up to 100 μM . However, upon illuminating with red light ($\lambda > 610\text{ nm}$), it shows substantial cytotoxicity with an IC_{50} value, defined as the dye concentration required to kill 50 % of the cells, of 0.55 μM (Fig. 2.4b, Table 2.2). The oxaliplatin analogue **2.17** exhibits cytostatic activity both in the absence and presence of light, and the corresponding IC_{50} values are 10.7 and 5.5 μM , respectively. It is interesting to note the enhanced cytotoxicity under illumination. The actual mechanism however remains elusive at this stage. Having a photosensitizer and a chemotherapeutic drug in the same molecule, conjugate **2.11** is highly photocytotoxic. The IC_{50} value is as low as 0.11 μM , which is five-fold lower than that of **2.14**. In fact, this conjugate is much more potent than the classical photosensitizer porfimer sodium, which has an IC_{50} value of 4.5 $\mu\text{g mL}^{-1}$ under the same experimental conditions (vs. 0.12 $\mu\text{g mL}^{-1}$ for **2.11**). Its cytotoxicity is also

Fig. 2.3 Comparison of the rate of decay of DPBF (initial concentration = 70 μM) sensitized by **2.11**, **2.14**, or ZnPc (all at 3 μM) in DMF as shown by the decrease in the absorbance at 411 nm



significantly higher than that of oxaliplatin and some of its derivatives, of which the IC_{50} values are in the range of $2\text{--}30\text{ }\mu\text{g mL}^{-1}$ [14]. Conjugate **2.11** also exhibits some dark toxicity ($IC_{50} = 78.5\text{ }\mu\text{M}$), which can be attributed to the oxaliplatin moiety as **2.14** is nontoxic under these conditions. As a better control, the cytotoxicity of an equimolar mixture of **2.14** and **2.17** was also studied and compared with that of **2.11**. It can be seen in Fig. 2.4b and Table 2.2 that the mixture is relatively more potent than **2.14** alone ($IC_{50} = 0.42$ vs. $0.55\text{ }\mu\text{M}$) probably due to the additional antitumor effect of the oxaliplatin derivative. However, its photocytotoxicity is still significantly lower than that of **2.11** ($IC_{50} = 0.42$ vs. $0.11\text{ }\mu\text{M}$). The results clearly show that the two antitumor components in conjugate **2.11** work in a cooperative fashion.

Considering the fact that the aggregation state of photosensitizers is an important factor relating to their photodynamic activities,[4–6] the aggregation behavior of conjugate **2.11** and the reference compound **2.14**, formulated with Cremophor EL, in the Dulbecco's modified Eagle's medium (DMEM) was

Fig. 2.4 (a) Comparison of the cytotoxic effects of **2.11** (squares), **2.14** (triangles), **2.17** (circles), and an equimolar mixture of **2.14** and **2.17** (stars) on HT29 cells in the absence (closed symbols) and presence (open symbols) of light ($\lambda > 610\text{ nm}$, 40 mW cm^{-2} , 48 J cm^{-2}). Data are expressed as mean value \pm standard error of the mean (S.E.M.) of three independent experiments, each performed in quadruplicate. Figure (b) shows the data for **2.11** (squares), **2.14** (triangles), and an equimolar mixture of **2.14** and **2.17** (stars) in the range up to $2.0\text{ }\mu\text{M}$. (The conditions for the present experiments have been described in Sects. 7.1.4 and 7.2.2. Experimental details regarding all in vitro studies in this thesis can be found in Chap. 7)

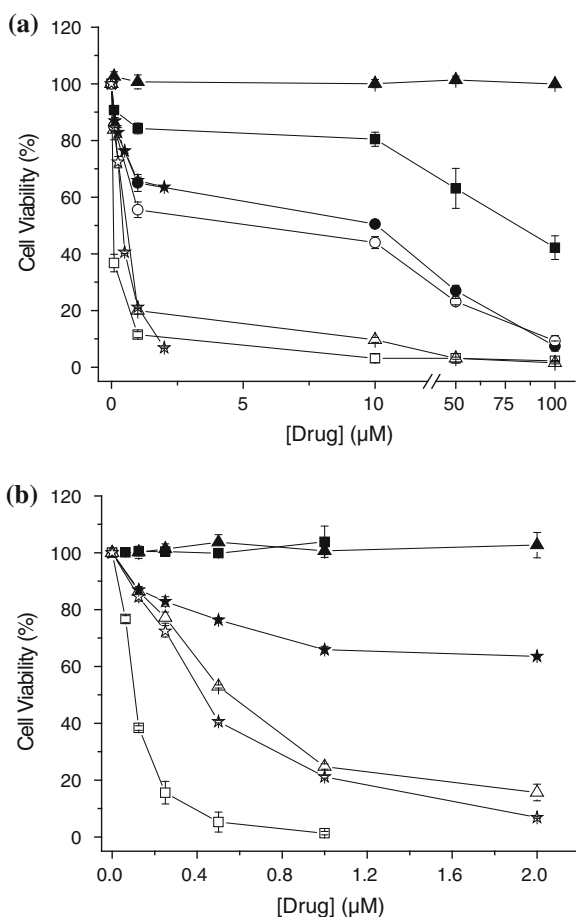


Table 2.2 IC₅₀ values for **2.11**, **2.14**, **2.17**, and an equimolar mixture of **2.14** and **2.17** against HT29 cells

Compound	IC ₅₀ ^d (μM)	
	In Dark	With Light
2.11	78.5	0.11
2.14	– ^e	0.55
2.17	10.7	5.5
1:1 mixture of 2.14 and 2.17	– ^f	0.42

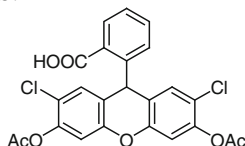
^d Defined as the dye concentration required to kill 50 % of the cells^e Non-cytotoxic up to 100 μM^f Not determined

examined by absorption and fluorescence spectroscopic methods. As shown in Fig. 2.5, both compounds show a relatively sharp and intense Q-band, and a relatively strong fluorescence emission. The results suggest that both compounds are not significantly aggregated under these conditions, which seems to be in accord with their high photocytotoxicity.

To account for the different photocytotoxicity of these two compounds, their cellular uptake was examined by fluorescence microscopy and absorption spectroscopy. As shown by the images captured by confocal laser scanning microscopy (Fig. 2.6a), both compounds could enter into the cells causing intracellular fluorescence after incubation for 2 h. The average relative fluorescence intensity per cell of these compounds was also measured and compared in Fig. 2.6b. It can be seen that the intracellular fluorescence intensity of **2.11** is about five-fold lower than that of **2.14**. However, to take into account that these two compounds may have different efficiency in generating fluorescence inside the cells, an extraction method was also employed to quantify the cellular uptake. After incubation with these phthalocyanines, the cells were washed and DMF was used to lyse the cells and extract the dyes. The dye concentrations inside the cells were quantified by measuring their Q-band absorbance at 672 nm. The results are depicted in Fig. 2.6c, which shows that the cellular uptake of **2.11** is actually about seven-fold higher than that of **2.14**. The presence of the oxaliplatin derivative in **2.11** may enhance the amphiphilicity of the overall compound, thereby promoting the cellular uptake. The higher cellular uptake of **2.11** is in accord with its higher photocytotoxicity.

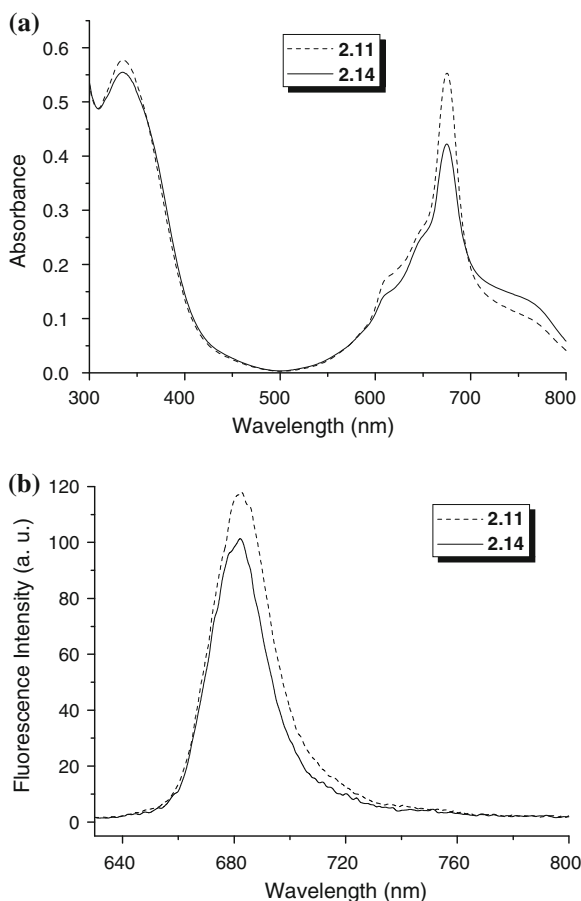
In addition, the intracellular production of ROS by these compounds was also studied using 2',7'-dichlorodihydrofluorescein diacetate (DCFDA) as the quencher [15]. DCFDA (see structure in the next page) is a fluorescent probe for visualizing oxidative stress in living cells. When DCFDA is taken up by cells, it undergoes deacetylation by esterase enzymes. Oxidation of the deacetylated product by the nearby ROS leads to the formation of 2',7'-dichlorofluorescein, which can be visualized with its strong emission at 525 nm when excited at 488 nm. There are two ways to produce intracellular ROS during the PDT process: (1) during PDT by the photosensitizer and (2) after PDT by the cells. In this study, by including DCFDA in the assay mixture during the illumination period, a direct production of

ROS by the drugs was demonstrated. As shown in Fig. 2.7, both **2.11** and **2.14** as well as the mixture of **2.14** and **2.17** can sensitize the production of ROS upon illumination. Conjugate **2.11** is the most efficient compound in producing intracellular ROS, which may be a result of its higher cellular uptake. Since the oxaliplatin derivative **2.17** is not a photosensitizer, it is expected that it does not produce any ROS even after illumination. The ROS production efficiencies of **2.14** and the mixture of **2.14** and **2.17** are therefore comparable to each other. All these results suggest that the higher photocytotoxicity of conjugate **2.11** can be attributed to its low aggregation tendency and higher cellular uptake and efficiency in generating intracellular ROS.



2',7'-dichlorodihydrofluorescein diacetate (DCFDA)

Fig. 2.5 (a) Electronic absorption and (b) fluorescence spectra ($\lambda_{\text{ex}} = 610 \text{ nm}$) of **2.11** (dashed line) and **2.14** (straight line), formulated with Cremophor EL, in the DMEM (both at $8 \mu\text{M}$)



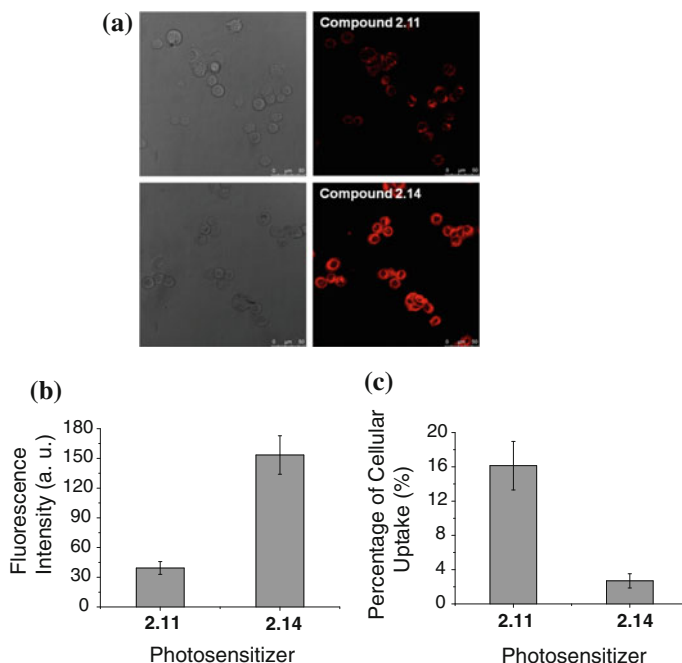
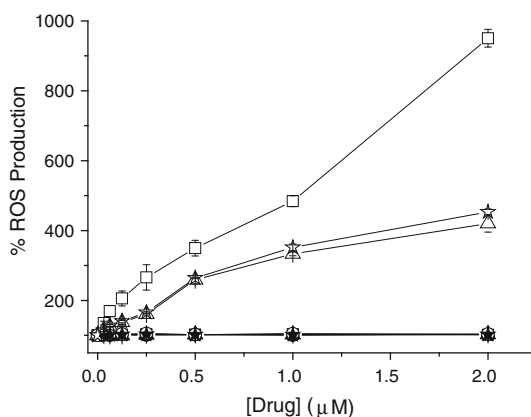


Fig. 2.6 (a) Confocal fluorescence images of HT29 cells after incubation with **2.11** or **2.14** for 2 h (both at 5 μ M). The corresponding bright field images are given in the left column. (b) Comparison of the relative intracellular fluorescence intensity of **2.11** and **2.14** (number of cells = 30). (c) Comparison of the percentage of cellular uptake of **2.11** and **2.14** as determined by an extraction method. Data are expressed as mean value \pm standard deviation (S.D.) of three independent experiments

Fig. 2.7 ROS production induced by **2.11** (squares), **2.14** (triangles), **2.17** (circles), and an equimolar mixture of **2.14** and **2.17** (stars) in HT29 cells in the absence (closed symbols) and presence (open symbols) of light ($\lambda > 610$ nm, 40 mW cm^{-2} , 48 J cm^{-2}). Data are expressed as mean value \pm S.E.M. of three independent experiments, each performed in quadruplicate



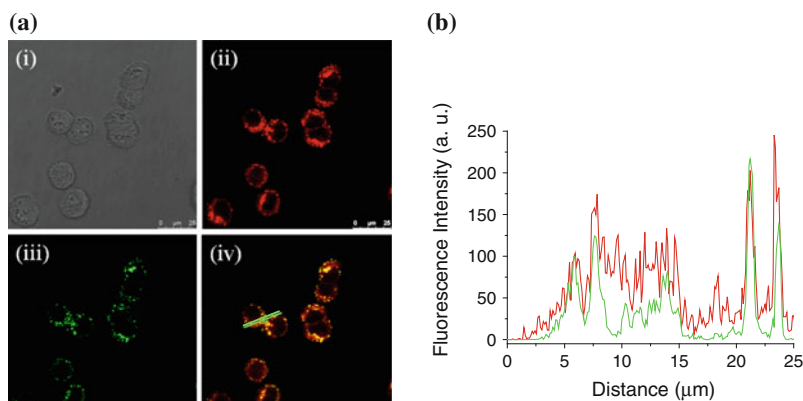


Fig. 2.8 (a) Visualization of (i) the bright field image, intracellular fluorescence of HT29 using filter sets specific for (ii) **2.11** (5 μM ; in red) and (iii) LysoTracker (in green), and (iv) the corresponding superimposed image. Figure (b) shows the fluorescence intensity profiles of **2.11** (red) and LysoTracker (green) traced along the green line in Figure (a) (iv)

The subcellular localization of conjugate **2.11** was also investigated. The cells were first incubated with the compound in the culture medium for 2 h, then stained with LysoTracker Green DND-26, ER-Tracker Green, MitoTracker Green FM, or SYTO-16 (for 10–20 min), which are specific dyes for lysosomes, endoplasmic reticulum, mitochondria, and nucleus, respectively. As shown in Fig. 2.8, the fluorescence caused by the LysoTracker (excited at 488 nm, monitored at 510–570 nm) can superimpose with the fluorescence caused by **2.11** (excited at 633 nm, monitored at 650–750 nm). The very similar fluorescence intensity line profiles of **2.11** and LysoTracker traced along the green line in Fig. 2.8a (iv) also confirms that **2.11** can target the lysosomes of the cells. By contrast, the fluorescence images of **2.11** could not be merged with those of the ER-Tracker, MitoTracker, and SYTO-16 (excited at 488 nm, monitored at 510–570 nm) (Fig. 2.9), showing that **2.11** is not localized in the endoplasmic reticulum, mitochondria, and nucleus of the cells.

It has been reported that PDT is a strong inducer of apoptosis in many situations [16]. The earliest hallmark of apoptosis is the loss of plasma membrane asymmetry. In apoptotic cells, the membrane phospholipid phosphatidylserine is translocated from the inner to outer leaflet of the plasma membrane, thus exposing phosphatidylserine to the external cellular environment. Annexin V-green fluorescent protein (GFP) has high affinity for phosphatidylserine and therefore serves as a sensitive probe for identifying apoptotic cells [17]. Generally, annexin V-GFP is costained together with propidium iodide (PI), which is a fluorescent probe to distinguish viable cells from dead cells, as the former with intact membranes exclude PI. We studied the mode of cell death induced by **2.11** by examining the

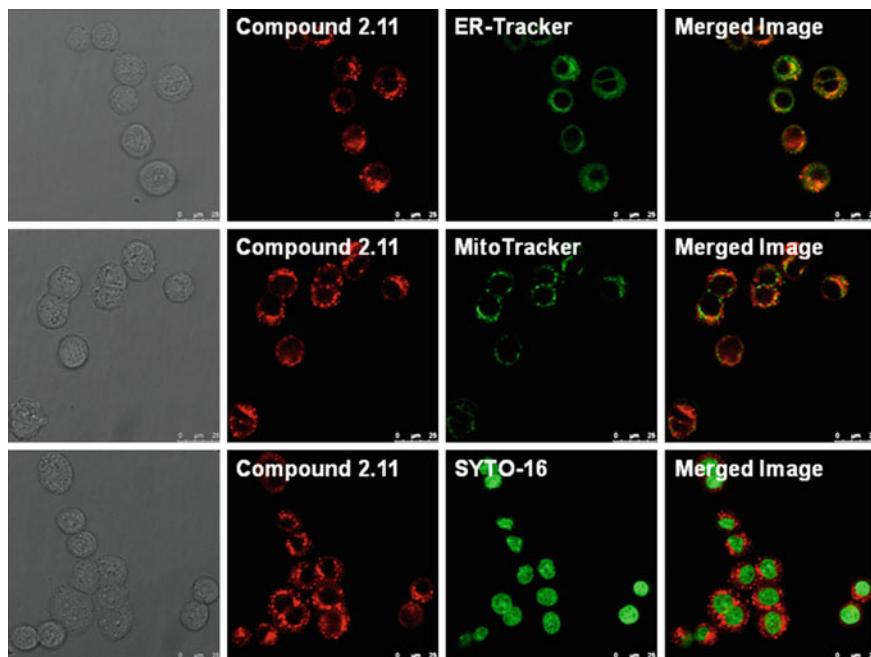


Fig. 2.9 Visualization of the bright field images (column 1), intracellular fluorescence of HT29 using filter sets specific for **2.11** (5 μ M; column 2, in *red*) and ER-Tracker, MitoTracker, or SYTO-16 (column 3, in *green*), and the corresponding superimposed images (column 4)

dual fluorescence of annexin V-GFP/PI using flow cytometry. In order to find out whether the introduction of the oxaliplatin derivative will alter the cell death mechanism, the results for **2.14** and **2.17** were also compared. The cell populations in different phases of cell death, namely viable (annexin V-GFP⁻/PI⁻), early apoptotic (annexin V-GFP⁺/PI⁻), and necrotic or late-stage apoptotic (annexin V-GFP⁺/PI⁺) were examined at the respective IC₅₀ values of the drugs. The only exception was for **2.14** in the dark for which the IC₅₀ value could not be determined, a dye concentration of 100 μ M was used for the measurements. As shown in Table 2.3, when the cells were treated with **2.11** or **2.14** in the presence of light, about 50 % of apoptotic cells and less than 10 % of necrotic cells were observed. Compound **2.11** also exhibited a significant dark toxicity, showing 41 % of apoptotic cells and 9 % of necrotic cells after the treatment due to the oxaliplatin derivative. For **2.14** in the dark, more than 95 % of the tumor cells remained viable even at 100 μ M. The oxaliplatin derivative **2.17** could induce apoptotic as well as necrotic cells, both in the absence and presence of light. The results showed that apoptosis is the major pathway for the PDT action of **2.11** and the presence of the oxaliplatin derivative does not significantly affect the cell death pathways.

Table 2.3 Flow cytometric analysis of the cell death mechanism induced by **2.11**, **2.14**, and **2.17** at their respective IC₅₀ values in the absence and presence of light ($\lambda > 610$ nm, 40 mW cm⁻², 48 J cm⁻²) on HT29 cells. Data are expressed as mean value \pm S.D. of three independent experiments

	Drug (μ M)	Illumination	Cell population (%)		
			Viable	Early apoptotic	Late apoptotic/necrotic
Blank	0	—	95.0 \pm 1.2	3.3 \pm 0.5	1.2 \pm 0.3
2.11	0.11	+	36.5 \pm 1.1	54.2 \pm 2.9	8.4 \pm 1.6
	78	—	48.9 \pm 1.5	41.0 \pm 1.2	9.3 \pm 0.7
2.14	0.55	+	44.9 \pm 1.9	50.2 \pm 1.9	4.4 \pm 0.7
	100 ^g	—	95.3 \pm 1.8	2.2 \pm 1.5	2.1 \pm 1.2
2.17	5.5	+	45.2 \pm 4.8	41.4 \pm 1.8	13.0 \pm 3.1
	10.7	—	53.8 \pm 3.5	25.7 \pm 3.0	19.9 \pm 0.6

^g The IC₅₀ value could not be determined

2.3 Summary

In summary, we have synthesized and characterized a zinc(II) phthalocyanine-platinum complex conjugate and evaluated its in vitro photodynamic activities. This conjugate contains both photo- and chemotherapeutic agents which are covalently linked and function in a cooperative manner. The introduction of the oxaliplatin derivative can enhance the cellular uptake and intracellular ROS generation efficiency of the phthalocyanine unit, resulting in a higher cytotoxicity. The IC₅₀ value of the conjugate is as low as 0.11 μ M toward the HT29 cells, which is five-fold lower than that of the reference compound without the oxaliplatin derivative. The conjugate also shows preferential localization in the lysosomes of the cells and induces cell death mainly through apoptosis. The overall results show that this conjugate is a highly promising antitumor agent for dual chemo- and photodynamic therapy.

References

1. Zuluaga, M.-F., Lange, N.: *Curr. Med. Chem.* **15**, 1655 (2008)
2. Wong, E., Giandomenico, C.M.: *Chem. Rev.* **99**, 2451 (1999)
3. Kelland, L.: *Nat. Rev. Cancer* **7**, 573 (2007)
4. Liu, J.-Y., Lo, P.-C., Fong, W.-P., Ng, D.K.P.: *Org. Biomol. Chem.* **7**, 1583 (2009)
5. Liu, J.-Y., Jiang, X.-J., Fong, W.-P., Ng, D.K.P.: *Org. Biomol. Chem.* **6**, 4560 (2008)
6. Liu, J.-Y., Lo, P.-C., Jiang, X.-J., Fong, W.-P., Ng, D. K. P.: *Dalton Trans.* **2009**, 4129 (2009)
7. Stein, A., Arnold, D.: *Expert Opin. Pharmacother.* **13**, 125 (2012)
8. Richard, A., Bourel-Bonnet, L.: *Chem. Eur. J.* **11**, 7315 (2005)
9. Loiseau, F.A., Hill, A.M., Hii, K.K.: *Tetrahedron* **63**, 9947 (2007)
10. Wyrick, S.D., Chaney, S.G.J.: *Labelled Compd. Radiopharm.* **25**, 349 (1988)
11. Erdem, S.S., Nesterova, I.V., Soper, S.A., Hammer, R.P.J.: *Org. Chem.* **73**, 5003 (2008)
12. Scalise, I., Durantini, E.N.: *Bioorg. Med. Chem.* **13**, 3037 (2005)

13. Maree, M.D., Kuznetsova, N., Nyokong, T.: *J Photochem. Photobiol. A* **140**, 117 (2001)
14. Al-Allaf, T.A.K., Rashan, L.J., Ketler, G., Fiebig, H.-H., Al-Dujaili, A.H.: *Appl. Organometal. Chem.* **23**, 173 (2009)
15. Shen, H.M., Shi, C.Y., Shen, Y., Ong, C.N.: *Free Radical Biol. Med.* **21**, 139 (1996)
16. Oleinick, N.L., Morris, R.L., Belichenko, I.: *Photochem. Photobiol. Sci.* **1**, 1 (2002)
17. Vermes, I., Haanen, C., Steffens-Nakken, H., Reutelingsperger, C.J.: *Immunol. Methods* **184**, 39 (1995)

Towards Dual and Targeted Cancer Therapy with Novel
Phthalocyanine-based Photosensitizers

Lau, J.T.F.

2013, XXII, 180 p., Hardcover

ISBN: 978-3-319-00707-6